Cloud Formation & Turbulence Generation by Galactic Spiral Shocks

SFR@50

Woong-Tae Kim (SNU)

Collaborators: Eve Ostriker (UMD)
Chang-Goo Kim (SNU)

- Spiral arms trace dust, gas, and young stellar populations.
- Many spiral arm substructures including OB star complexes, gaseous spurs (feathers), and giant clouds

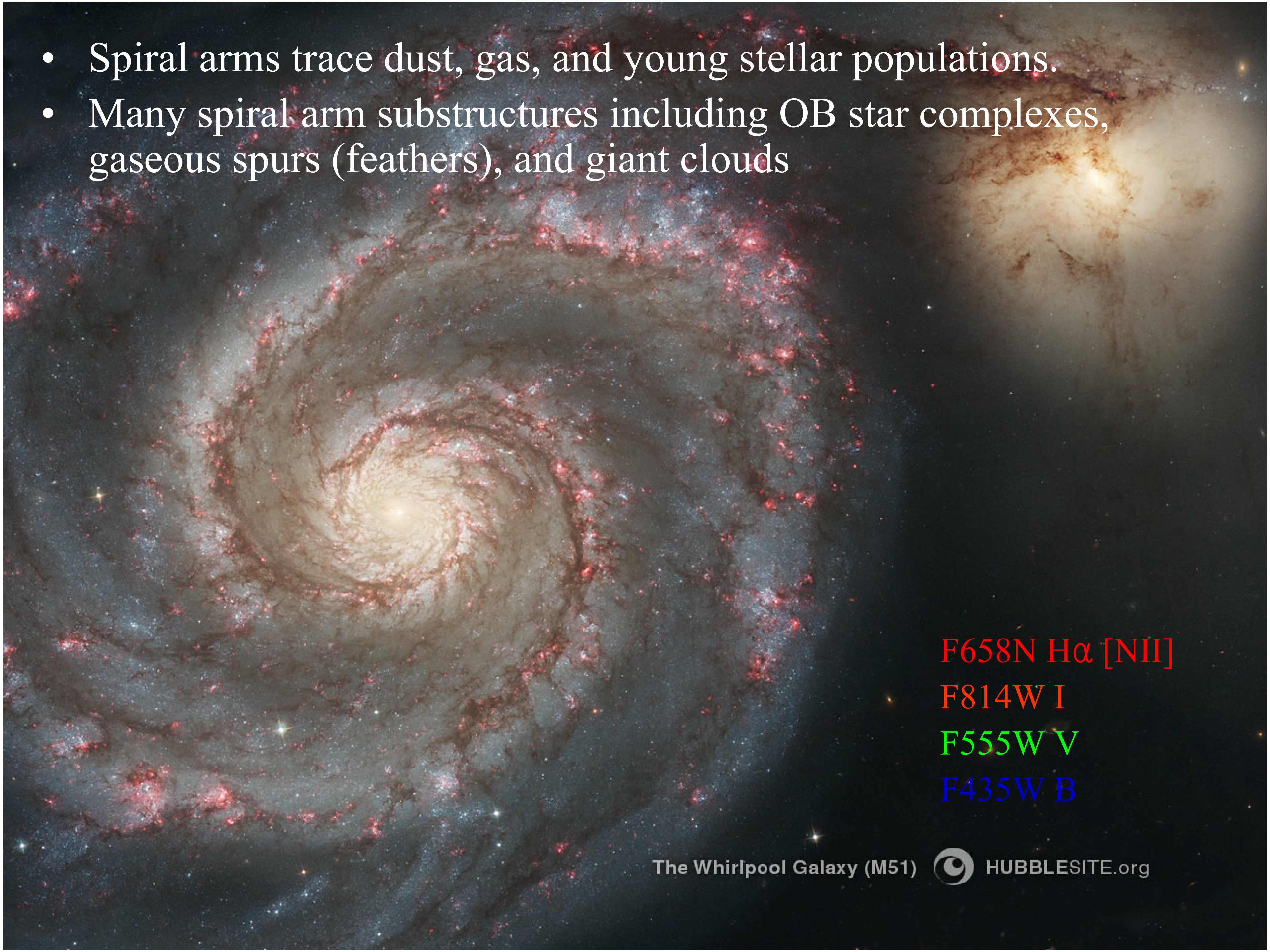

Giant Clouds

- Constitute perhaps a upper end of the GMC mass spectrum (when atomic envelopes are included).
- Typically, ~10^7 $M_\odot$ in mass and ~1 kpc in separations

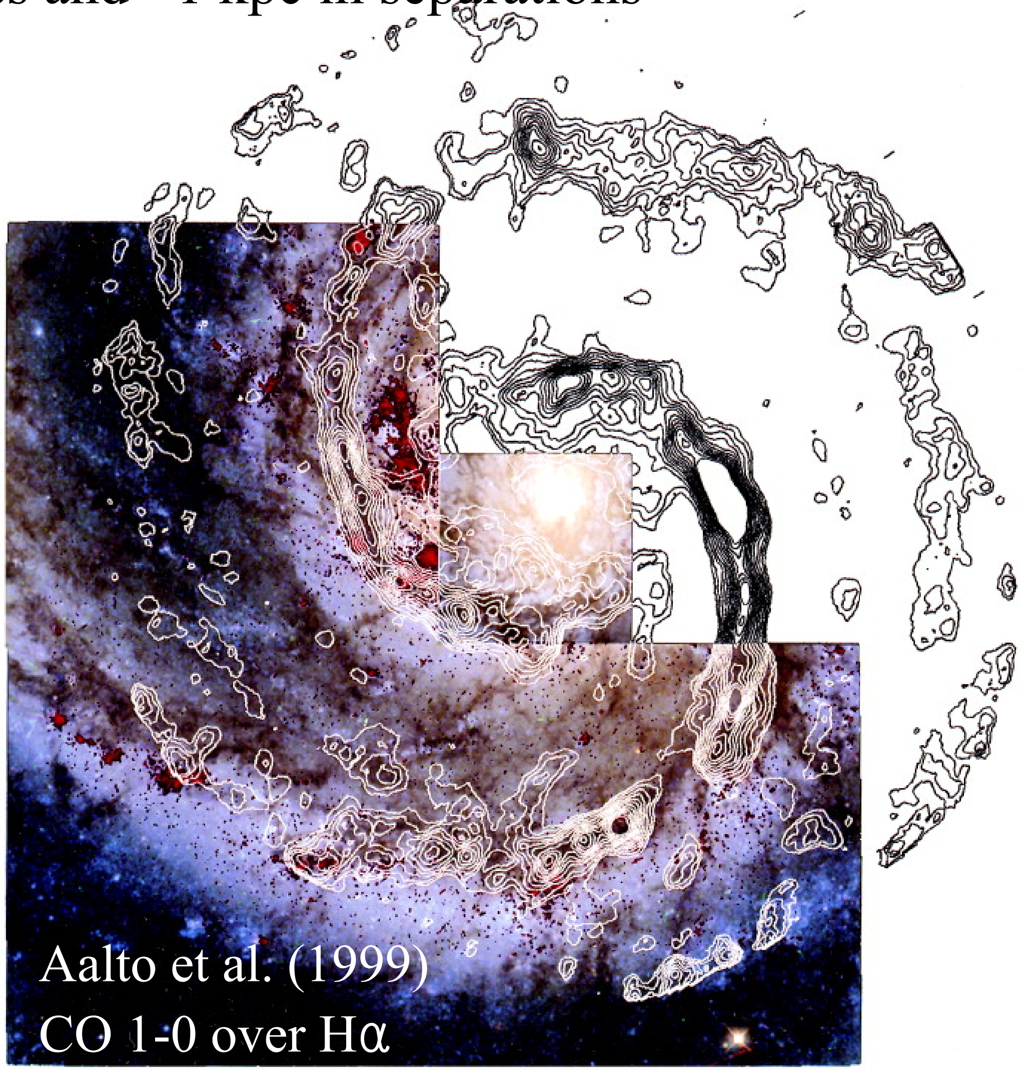

Gaseous Spurs/Feathers

- Prominent extinction features which emerge from a spiral arm dust lane and arch into the interarm region.
- Common in Sb and Sc galaxies (La Vigne et al. 2006)
- Corder et al. (2008) used the OVRO to map CO emission from spurs in M51
  - Distances of spurs from the arms: ~ 0.5 kpc
  - Masses of spurs : 2-5 × 10^6 $M_\odot$ each
- CARMA observations show that spur separation increases as the gas surface density decreases (La Vigne & Vogel 2009).

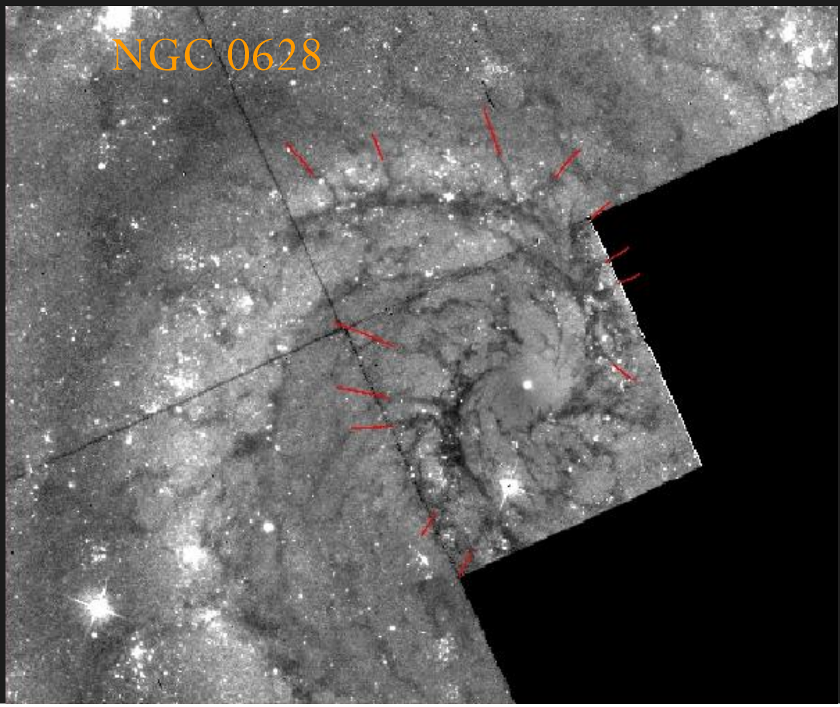

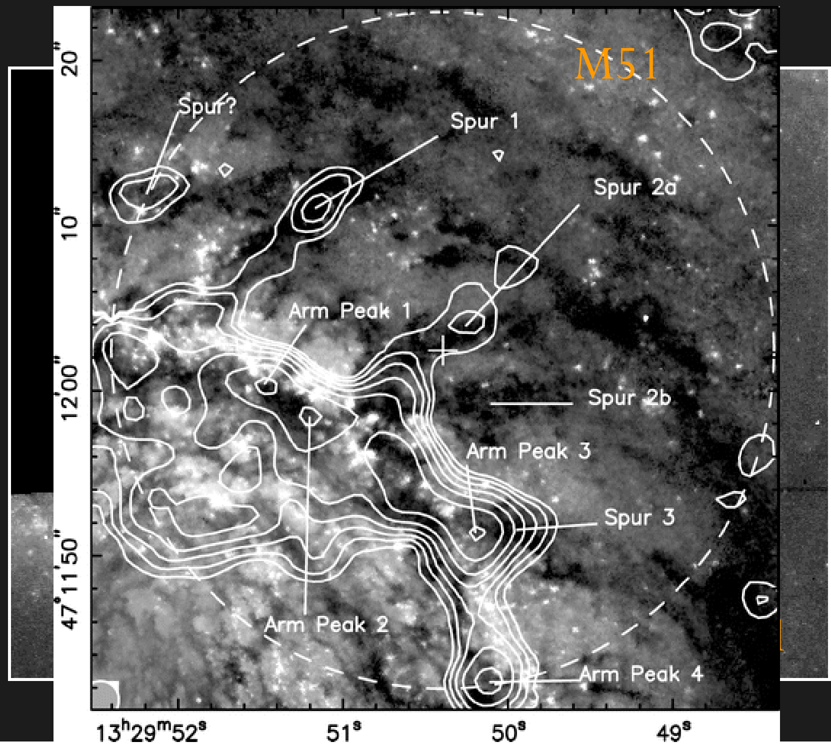

ISM Turbulence

- Turbulence in the ISM appears to be pervasive and highly supersonic.
  - $\sigma \sim 7$ km s^{-1} for both warm and cold HI gas near the Sun (Heiles and Troland 2003)
  - $\sigma_z \sim$ 6-10 km s^{-1} for external face-on galaxies, insensitive to galactocentric radius and spiral-arm phase (Dickey et al. 1990; van Zee & Bryant 1999; Petric & Rupen 2007)

- Driving sources (Elmegreen & Scalo 2004; Mckee & Ostriker 2007)
  - Stellar sources such as SN explosions and HII regions
    - Energy budget is right.
    - But, turbulence level is uncorrelated with star formation
  - Non-stellar sources such as magnetorotational instability, gravitational instability, thermal instability, spiral shocks, etc.
    - Observations indicate that the level of ISM turbulence is uncorrelated with star formation (e.g., van Zee & Bryant 1999; Petric & Rupen 2007)
    - Transport some of the kinetic energy in galaxy rotation into random gas motions.

Local Spiral Arm Coordinates

- Transfer to a frame corotating at $\Omega_p = \Omega_0/2$ with an arm, and erect a local "spiral coordinate system" (Roberts 1969; Shu et al. 1973).

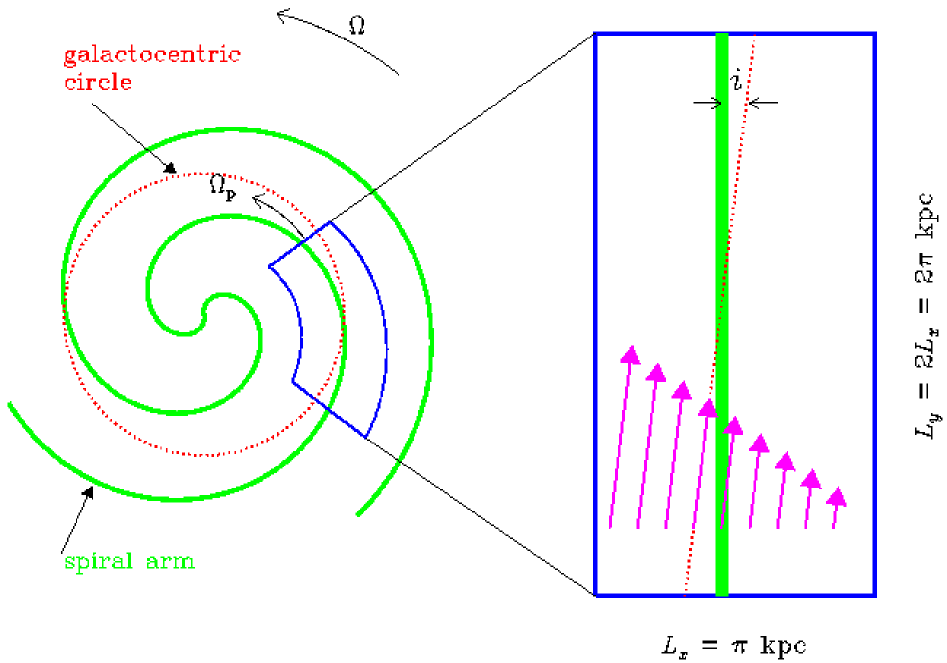

- Shearing-periodic boundary conditions
- External spiral potential:

$$\Phi_{ext} = \Phi_0 \cos(2\pi x / L_x)$$

$$F \equiv 2|\Phi_0| / (\Omega_0^2 R_0^2 \sin i)$$

1D Isothermal Spiral Shock

- Isothermal EOS with c_s=7-10 km s^{-1}
  - Corresponds to warm gas
  - Or, can be regarded as an "effective" velocity dispersion of the ISM including the turbulent contribution (Koyama & Ostriker 2009).
- 1D isothermal shocks are readily stationary
  - Represent stable equilibria.
- Shock compression implies strong magnetic fields and reversed shear inside spiral arms.
- Dense gas becomes less dense as it passes through the postshock expansion zone.

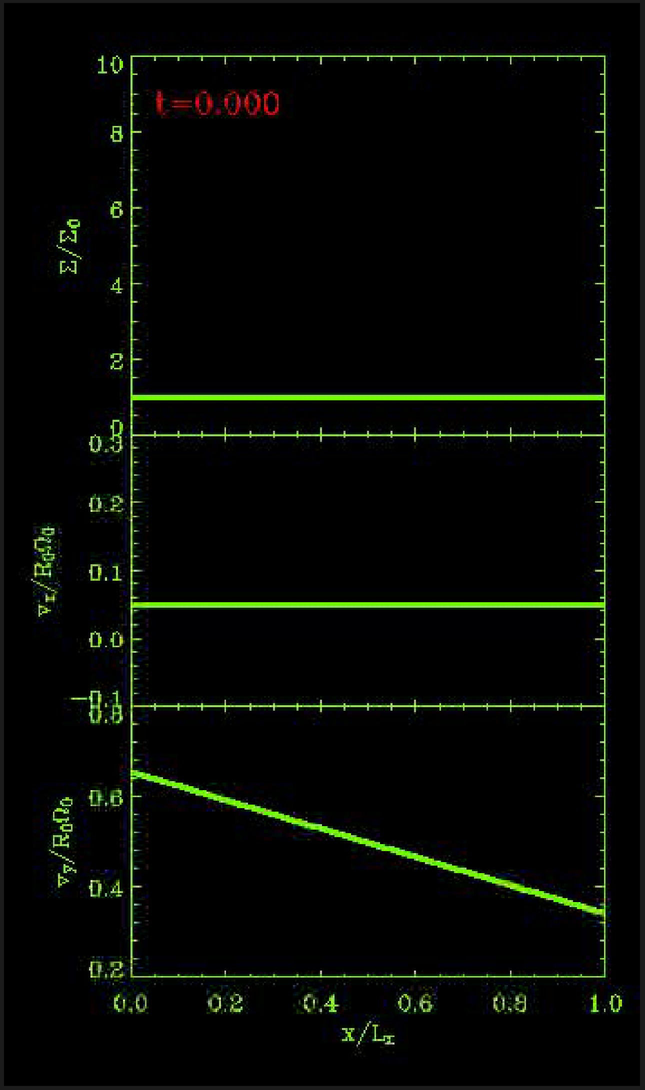

F=10%

Self-gravitating Mechanisms

Swing Amplifier Goldreich & Lynden-Bell (1965); Julian & Toomre (1966)		Magneto-Jeans Instability (MJI) Lynden-Bell (1966); Elmegreen (1987); Kim & Ostriker (2001)
Conspiracy among shear, Coriolis force, and self-gravity	Physical mechanism	Tension force from B-fields removes the stabilizing effect of Coriolis force.
required	Self-gravity	required
strong	**Velocity shear**	**weak**
stabilizing	**B-fields**	**de-stabilizing**
clouds ($\sim 10^7 M_\odot$)	outcomes	spurs + clouds ($10^7 M_\odot$)
3-4 orbits	Growth time	$\sim$ 1 orbits

Magnetized Spiral Arms

- Small net velocity shear and stronger magnetic fields inside spiral arms provide a favorable condition for the magneto-Jeans instability to develop (Elmegreen 1994; Kim & Ostriker 2002).
- Separation of gaseous spurs:
  - $L \sim (2\text{-}3)\ \lambda_{J,sp}$ in a razor thin disk.
- Masses of bound clumps:
  - $M \sim 4\times10^6\ M_\odot$ in a razor thin disk

    $\sim$ Jeans mass at the arm peak.

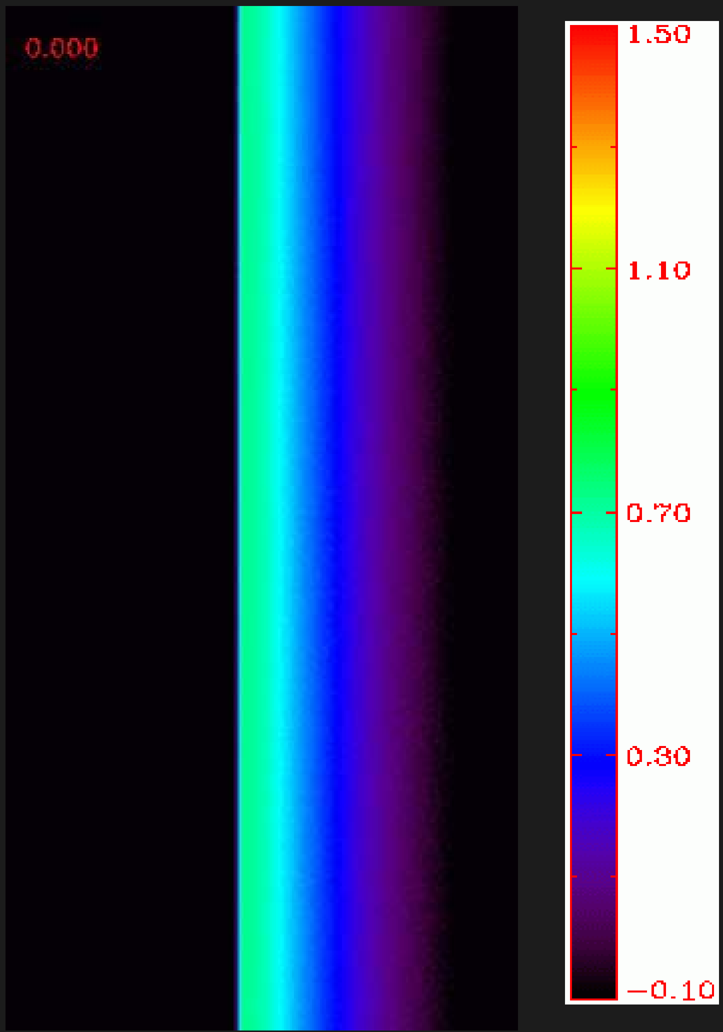

F = 3%, Q_0 = 1.5, β_0 = 1 $\mathrm{Log}_{10}(\Sigma/\Sigma_0)$

<Infinitesimally thin-disk>

Effect of Disk Stratification

- When vertical degrees of freedom are allowed, spiral shocks become non-stationary, swaying loosely back and forth in the direction perpendicular to the arm.
  - In sharp contrast to 1D cases where spiral shocks are readily stationary.
  - XZ flapping motions arises primarily because the arm-to-arm crossing periods are incommensurable with the vertical oscillation periods.

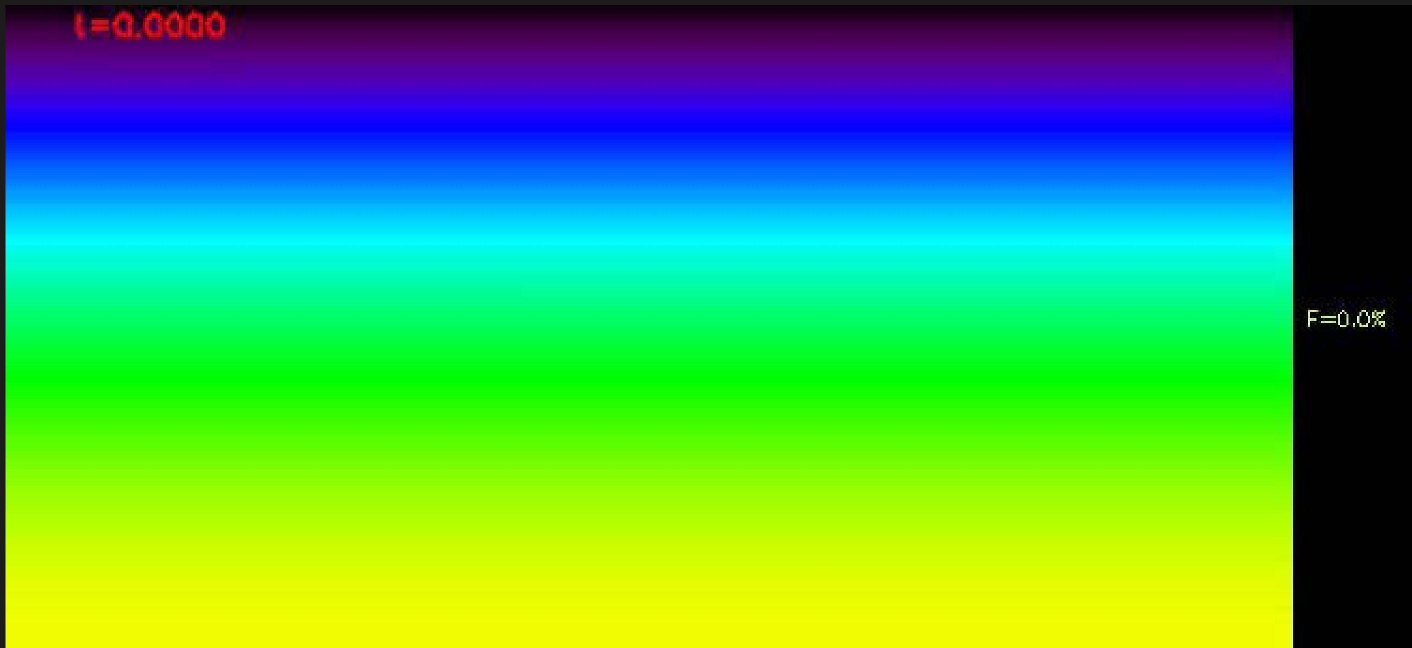

Kim, Kim, & Ostriker (2006)

$F = 10\%$, $Q = 2.0$, $\beta = 10$

Turbulence Driving by Spiral Shocks

- Shock flapping motions in the XZ plane are able to feed random gas motions in both arm and interarm region.
  - Velocity dispersions inside arms are larger than those in interarm regions by a factor of 2.
  - Despite strong shock dissipation, the induced motions persist at ~7-10 km s^{-1}.
  - Can be a substantial source of the interstellar turbulence.

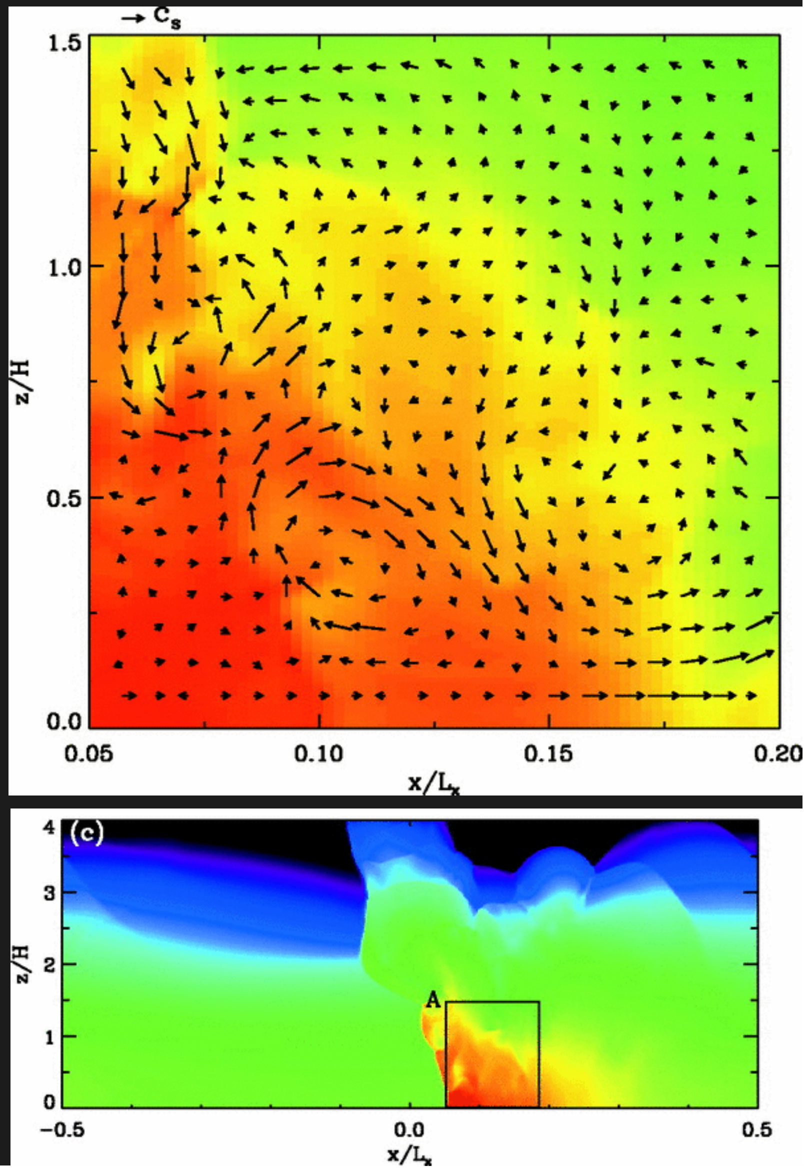

Magnetized 3D Spiral Arm

- 3D models still form spurs via Magneto-Jeans instability, although the reduced self-gravity in 3D produces less number of spurs.
- $\lambda_{spur} \sim 10\ \lambda_{J,\ arm}$, consistent with the results of La Vigne et al. (2006)
- $M_c = (1\text{-}3) \times 10^7\ M_{\odot}$, similar to the masses of observed giant clouds.

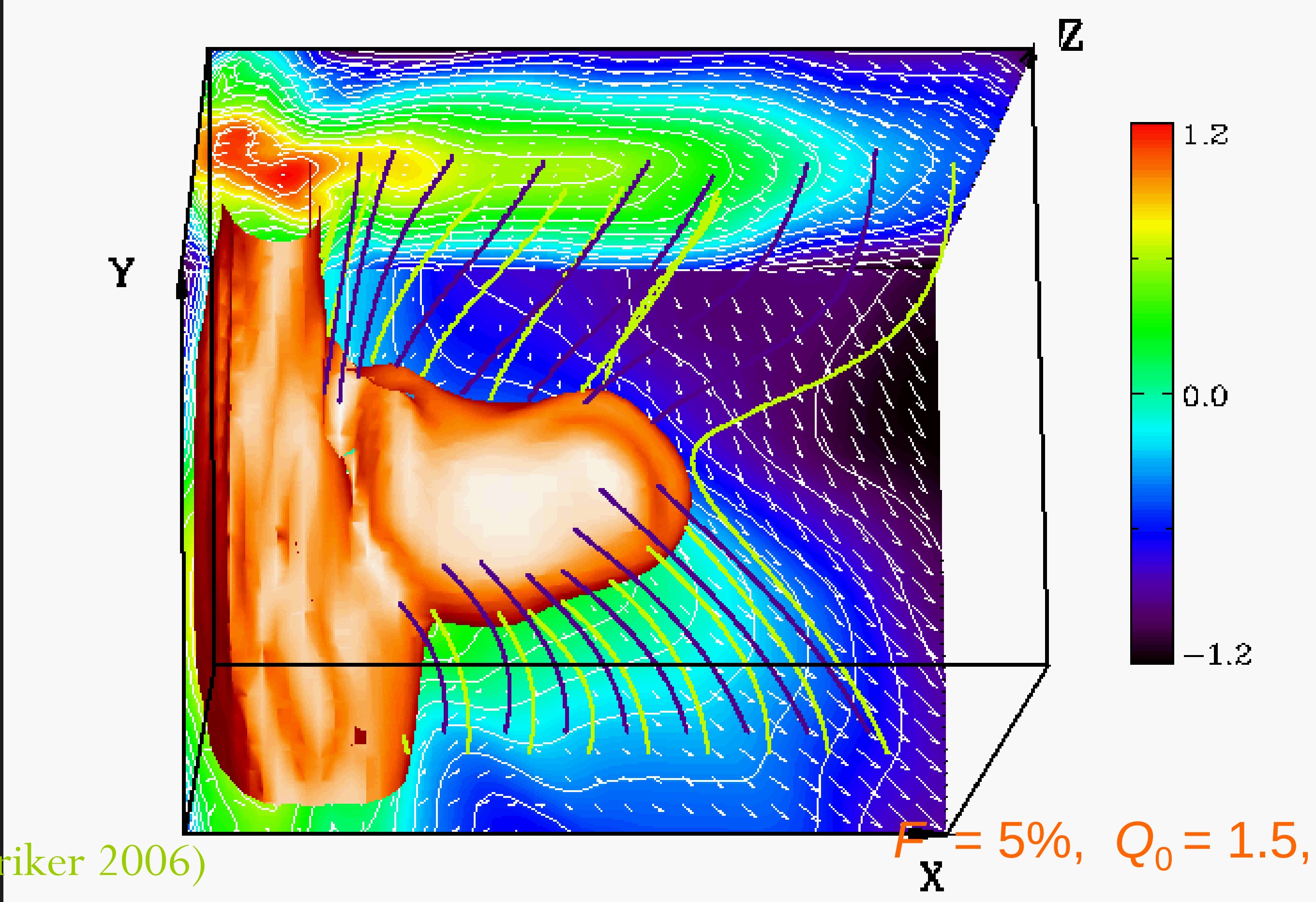

(Kim & Ostriker 2006)

$F = 5\%,\ \ Q_0 = 1.5,\ \beta_0 = 10$

Global Models

- Shetty & Ostriker (2006, 2008) ran global simulations and showed that spurs form due to magneto-Jeans instability when spiral arms are sufficiently strong.
- Wada & Coda (2004) proposed that a wiggle instability is another mechanism to form gaseous spurs.
- Dobbs & Bonnell (2006) & Dobbs (2008) showed that giant clouds and spurs form, even without gravity, by orbit crowding (or coalescence) of cold gas.

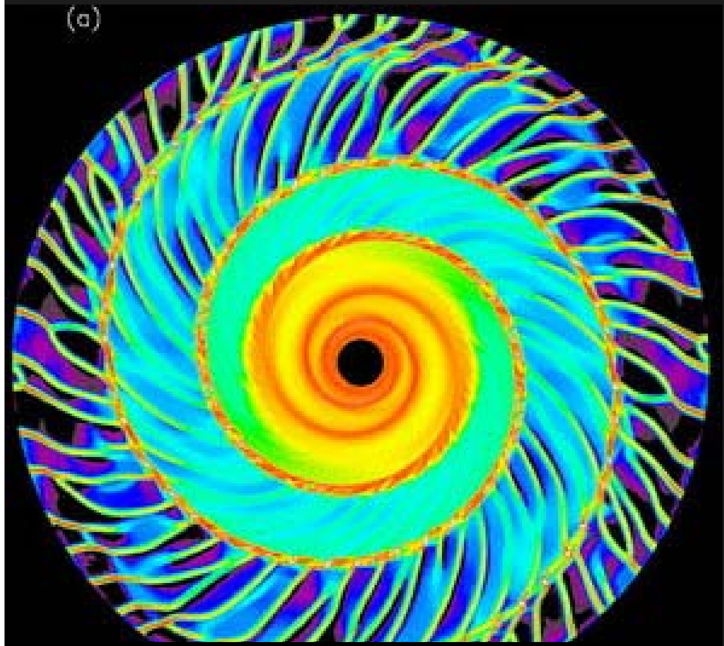

Shetty & Ostriker (2006)

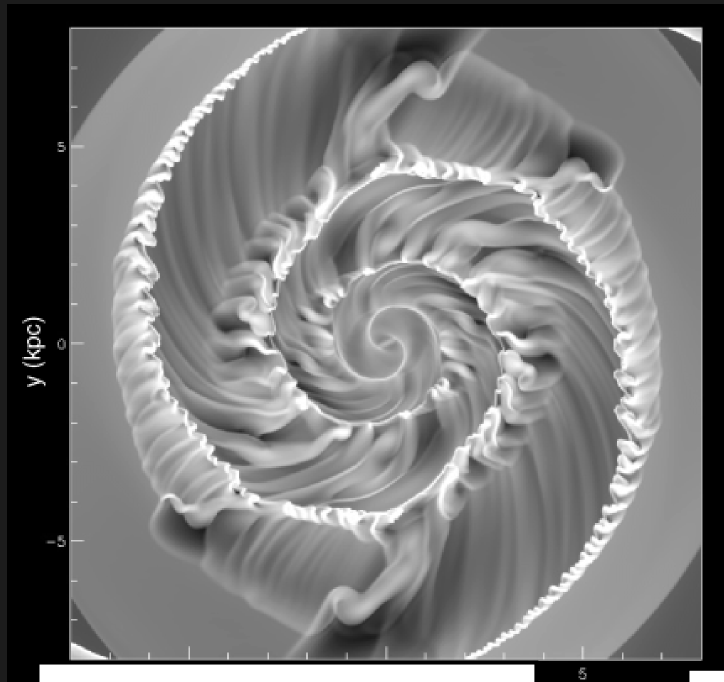

Wada & Koda (2004)

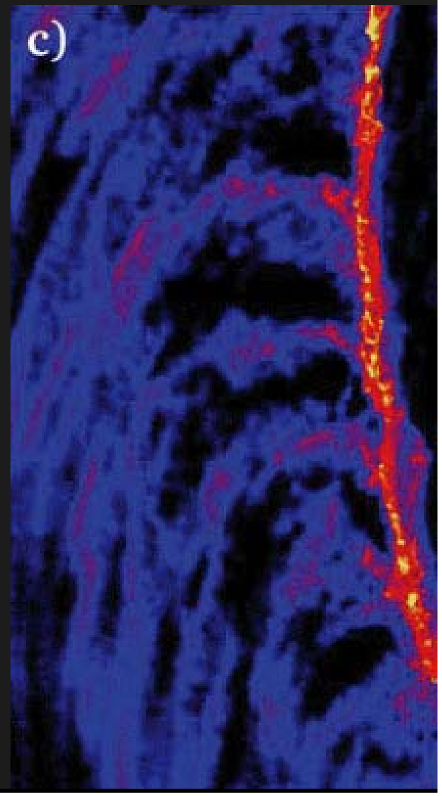

Dobbs & Bonnell (2006

Spiral Shocks with Thermal Instability

- The ISM is in general clumpy as a result of thermal instability (TI) (Field et al. 1969, Mckee & Ostriker 1977)
- Some previous work did not solve TI explicitly
  - Steady-state phase transition (Shu et al. 1972)
  - predefined two stable phase (Dobbs & Bonnell 2007)
  - poor resolution (Tubbs 1980; Marochnik et al. 1982)
- Global models with TI (Dobbs et al. 2008)

- 1D High resolution simulations
  - N=16,384 zones for 1D models ($\Delta x \sim 0.04$pc)
  - ATHENA code (Gardiner & Stone 2005, 2007)
    - single step, second-order Godunov scheme
  - Cooling and conduction solver (Piontek & Ostriker 2004)
    - cooling function (Koyama & Inutsuka 2002; Wolfire et al. 2003; Vazquez-Semadeni 2007)
    - thermal conductivity at $\kappa = 10^5$ erg cm^{-1} K^{-1} s^{-1}

1D Model

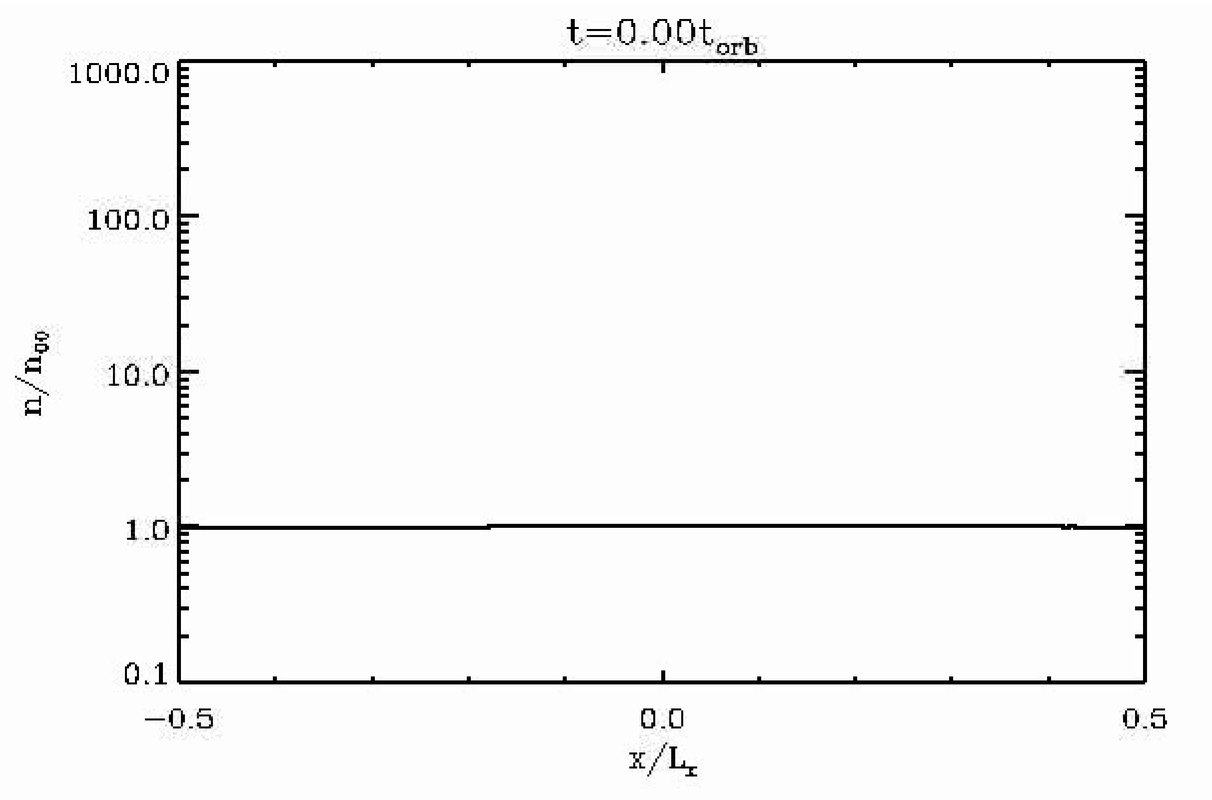
t=0.00t_orb
1000.0
100.0
10.0
1.0
0.1
n/n_00
−0.5
0.0
0.5
x/L_x

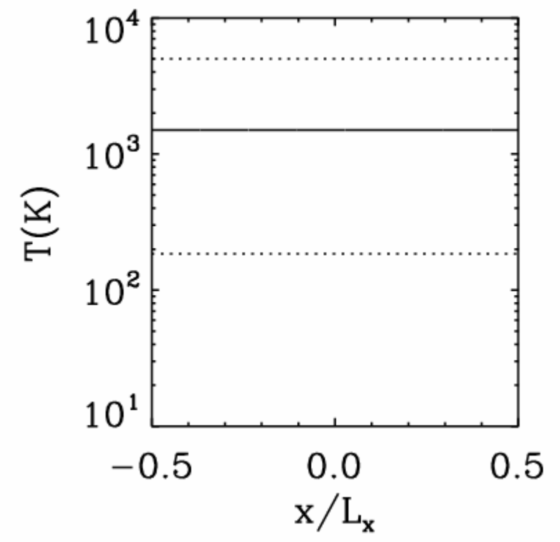
10^4
10^3
10^2
10^1
T(K)
−0.5
0.0
0.5
x/L_x

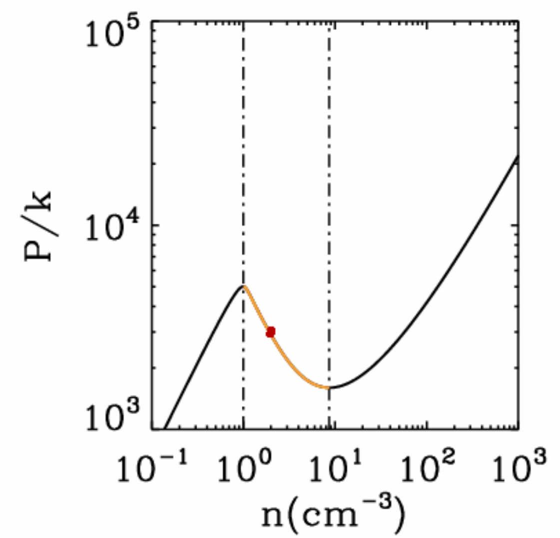
10^5
10^4
10^3
P/k
10^-1
10^0
10^1
10^2
10^3
n(cm^-3)

1D Model

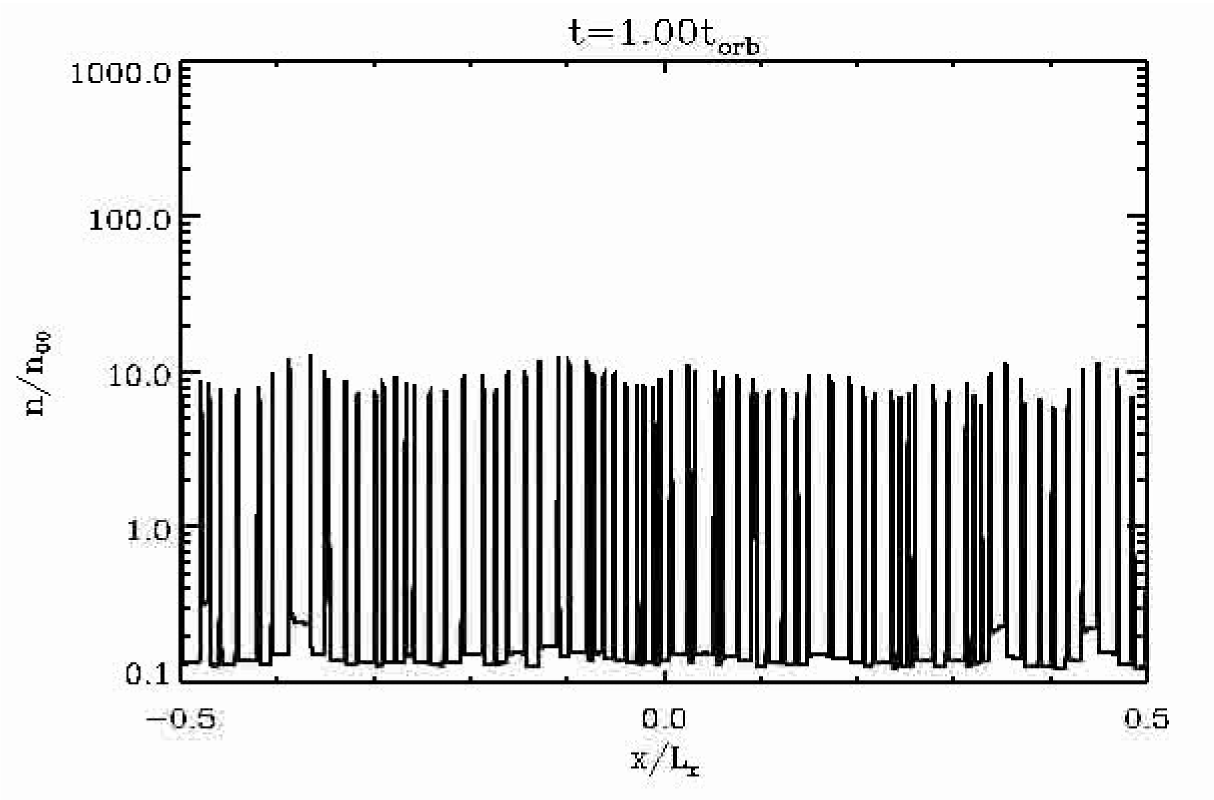

t=1.00t_orb
1000.0
100.0
10.0
1.0
0.1
n/n_00
−0.5
0.0
0.5
x/L_x

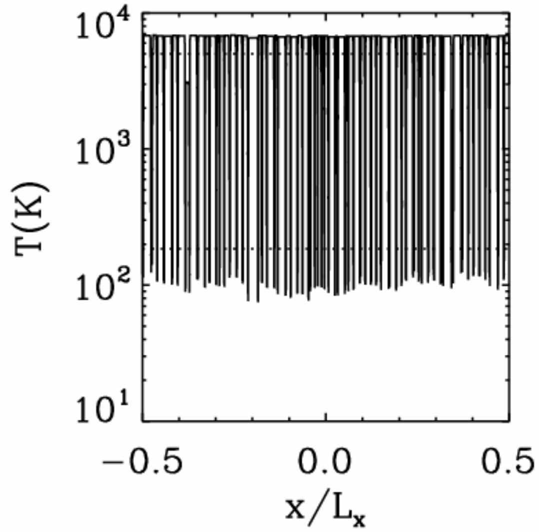

T(K)
x/L_x
−0.5
0.0
0.5

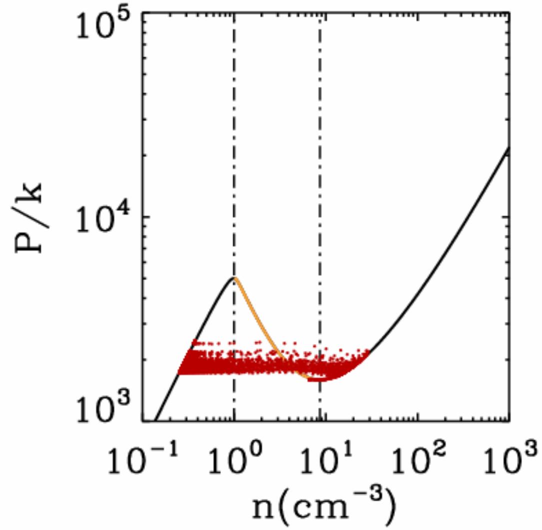

P/k
n(cm^-3)

1D Model

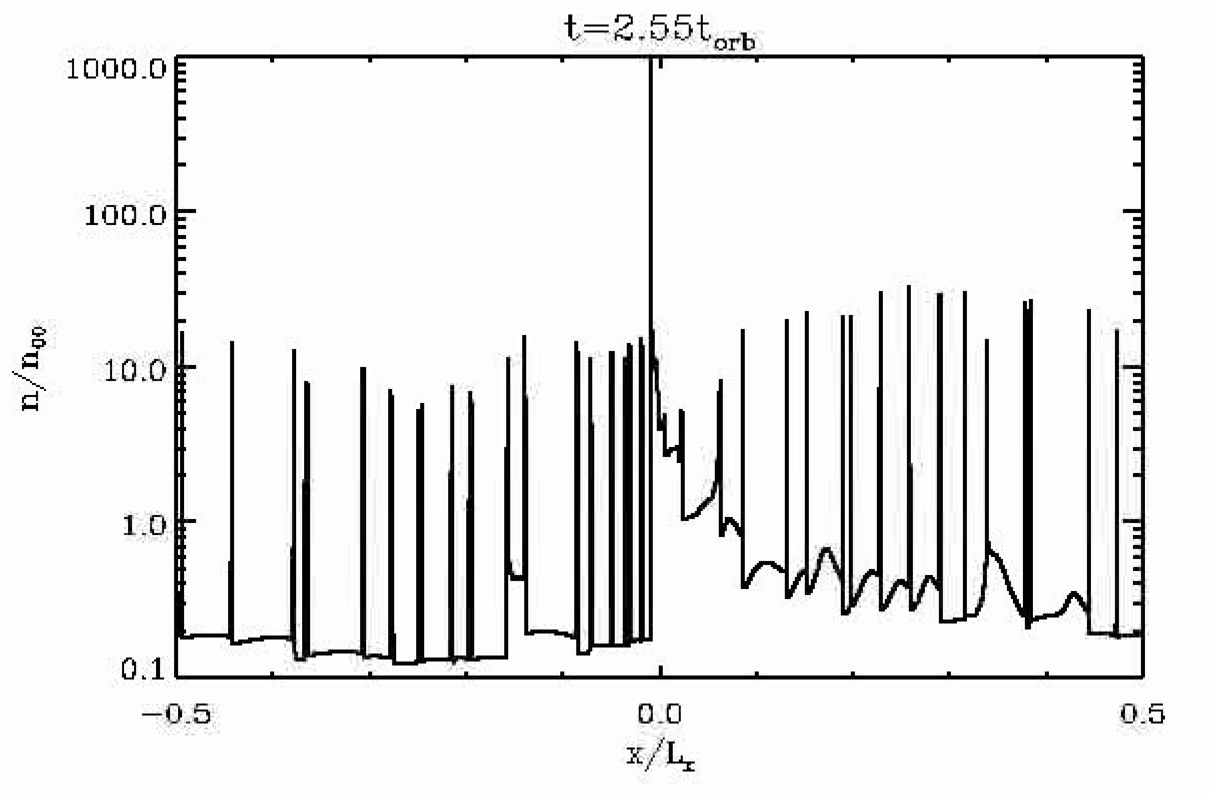

t=2.55t$_{orb}$
1000.0
100.0
10.0
1.0
0.1
n/n$_{00}$
−0.5
0.0
0.5
x/L$_x$

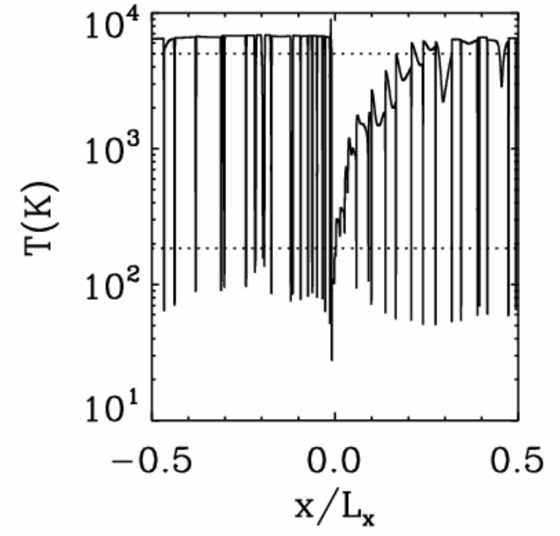

10^4
10^3
10^2
10^1
T(K)
−0.5
0.0
0.5
x/L$_x$

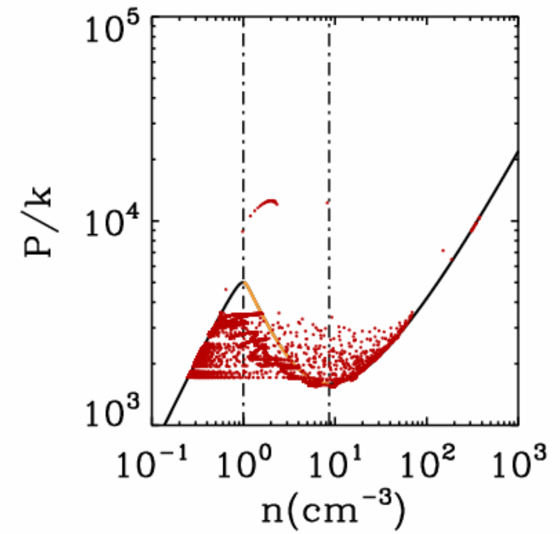

10^5
10^4
10^3
P/k
10^{-1}
10^0
10^1
10^2
10^3
n(cm^{-3})

1D Model

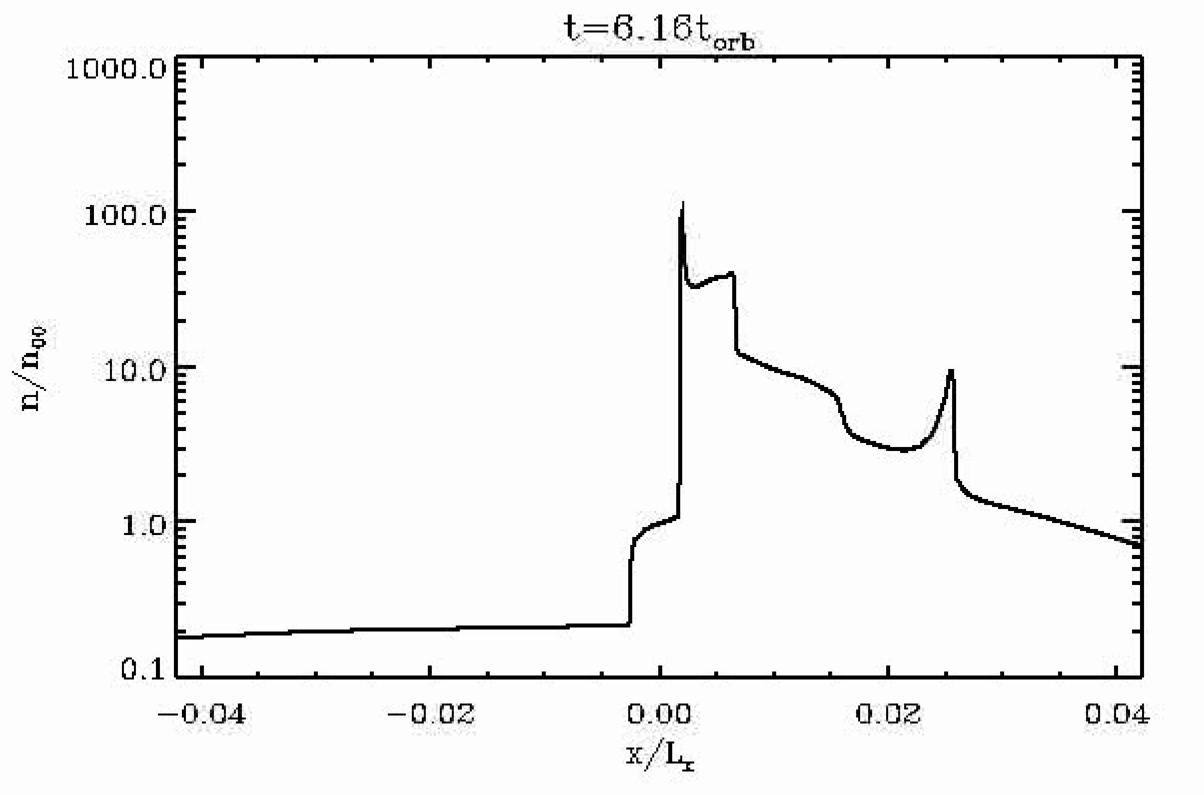

t=6.16t_orb
1000.0
100.0
10.0
1.0
0.1
n/n_00
-0.04
-0.02
0.00
0.02
0.04
x/L_x

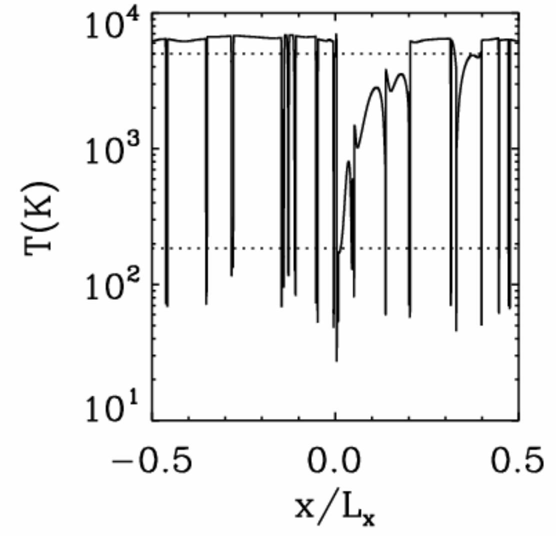

10^4
10^3
10^2
10^1
T(K)
-0.5
0.0
0.5
x/L_x

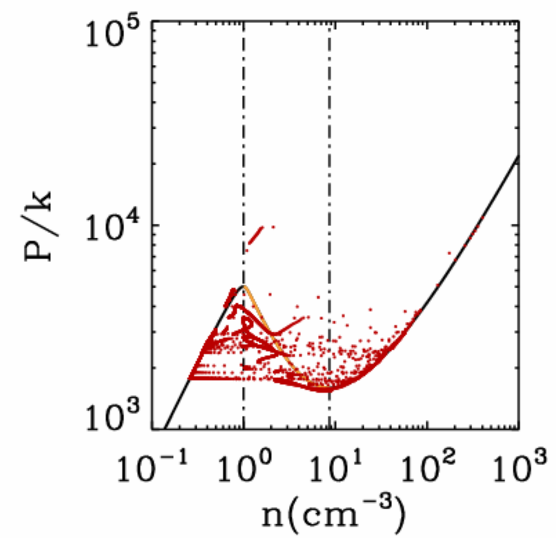

10^5
10^4
10^3
P/k
10^-1
10^0
10^1
10^2
10^3
n(cm^-3)

1D Spiral Shock with TI

(Kim, Kim, & Ostriker 2008)

- 1D Spiral shocks are in quasi-steady state.
- Phase transitions occurs
  - from warm to cold at the shock front
  - from cold to warm at the transition zone behind the shock ($\Delta x/L_x \sim 16\%$; $\tau/t_{orb} \sim 22\%$)
- Gas at intermediate-temperature represents ~25-30% of the total mass
- Random gas motions driven by a spiral shock with TI amount to about 1.5 km s^{-1}
  - About 5-7 times larger than in pure TI (Kritsuk & Norman 2002; Piontek & Ostriker 2004)

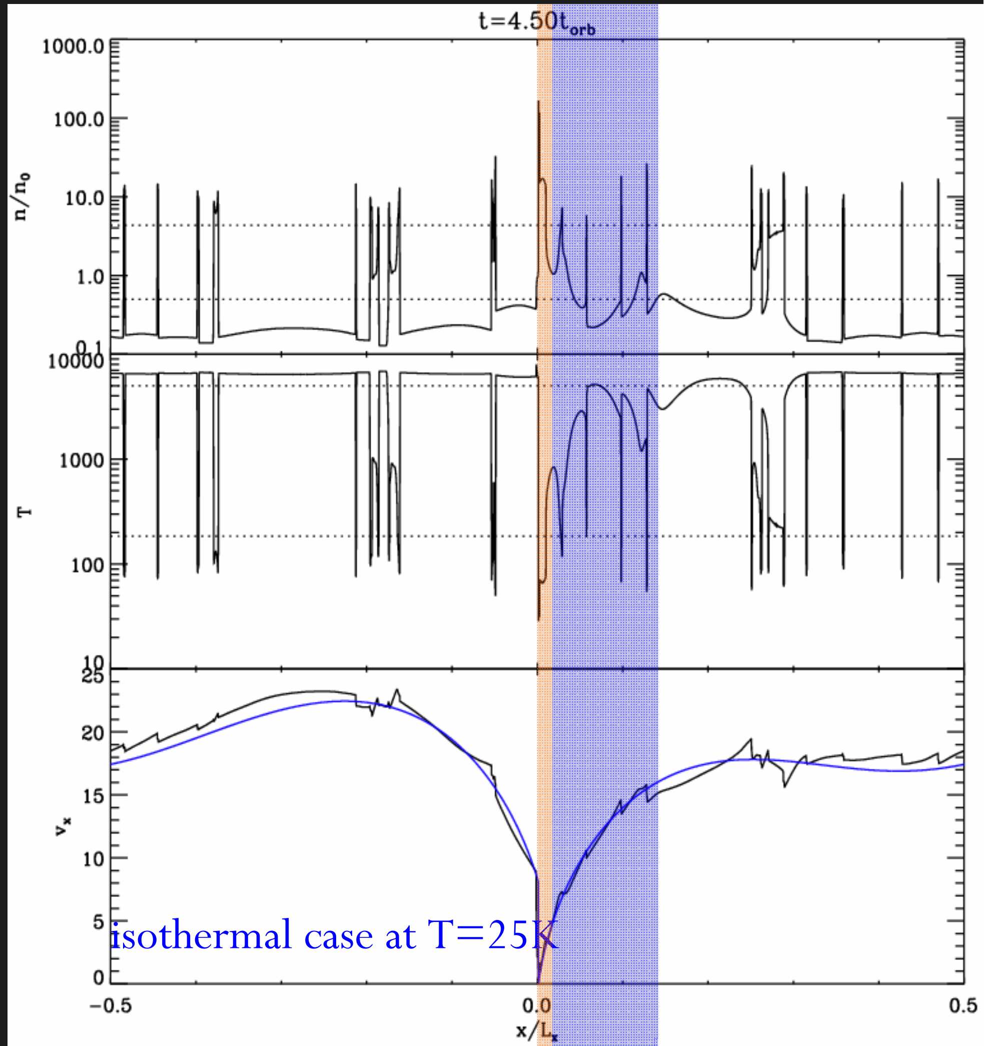

2D Spiral Shocks with TI

(Kim, Kim, & Ostriker, in preparation)

- Cooling and heating
  - Original EOS: simple fitting formula (Koyama & Inutsuka 2002)
  - Modified EOS: additional heating for large density
    - Mimic SF feedback in a very simple way

$$\Gamma = \Gamma_0 \exp[(n/n_0)^3]$$

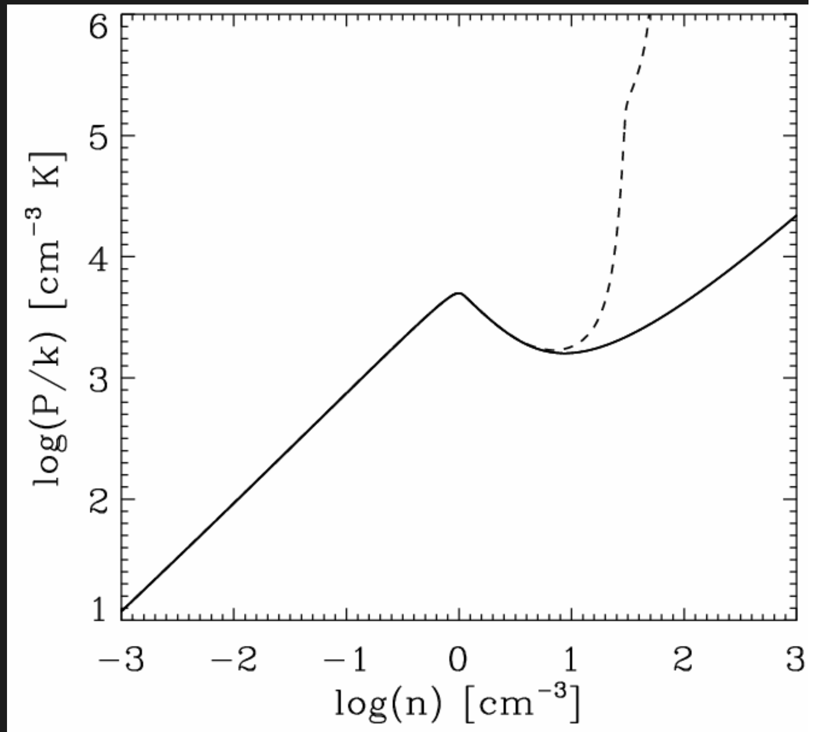

- Models: (F=5%; Σ = 10 $M_\odot pc^{-2}$)
  - A: no gravity, original EOS
  - B: no gravity, modified EOS
  - C: with gravity, modified EOS

Model A (Original EOS, no Gravity)

- F=5%, Σ=10$M_{\odot}$ pc^{-2}, without self-gravity
- Initially, the disk collapses toward the midplane because of strong cooling.
- Spiral shocks develop in response to an imposed spiral potential.
  - Allow phase transitions
  - Exhibit flapping motions

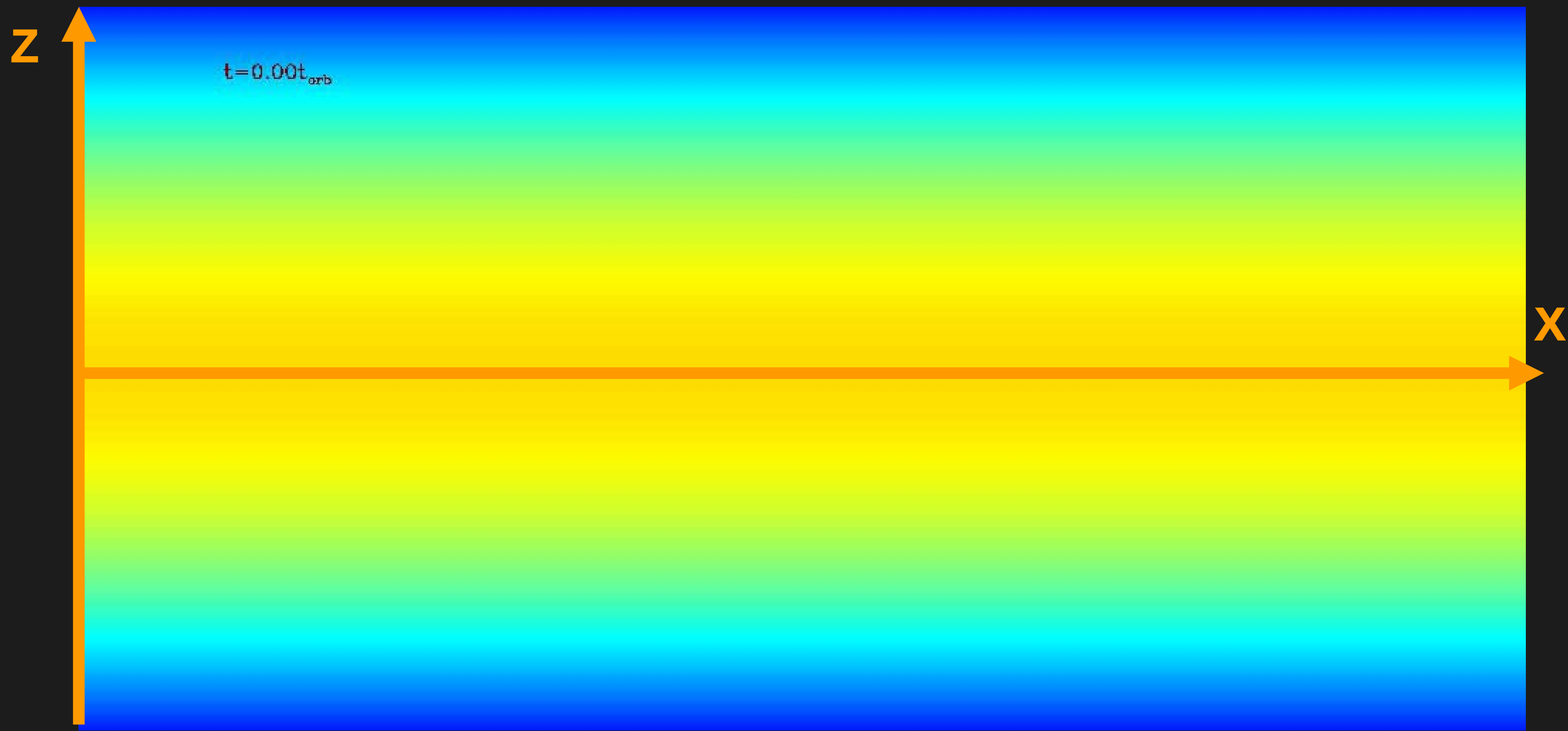

Model Comp

- Dense gas is confined to a thin layer:
  - H = 50-60 pc (model A)
  - H = 60-70 pc (model B)
  - H = 40-60 pc (model C)
  - Similar to the results of Dobbs et al. (2008)
- Models even without self-gravity form clumps that are bounded by thermal pressure.
  - Shocked gas has so large density to remain dense even after passing the expansion zone.
  - Similar to the results of Dobbs (2008) and Dobbs et al. (2008)
  - $M \sim 10^5 M_\odot$ (if spherical shape is assumed)
- Clumps in models with self-gravity
  - self-gravitating: $\alpha_{vir} \sim 2$ (KE ~ PE)
  - $M \sim 10^6 M_\odot$ (if spherical shape is assumed)

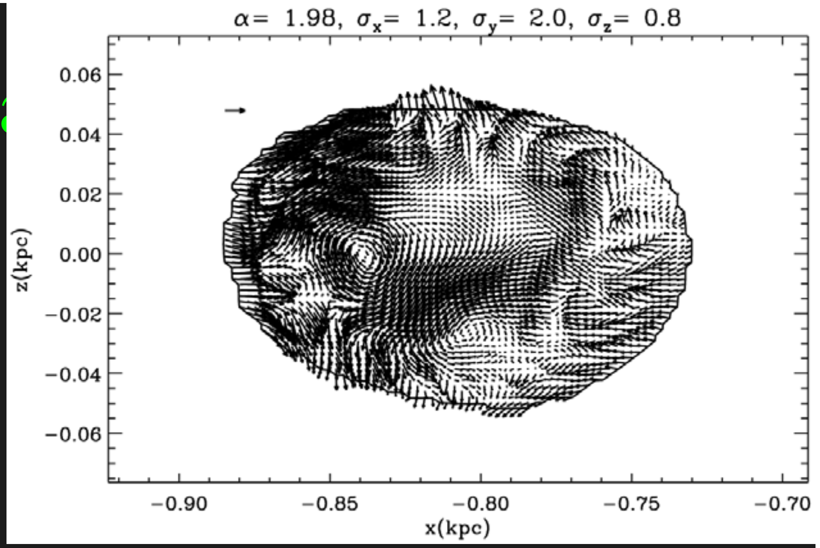

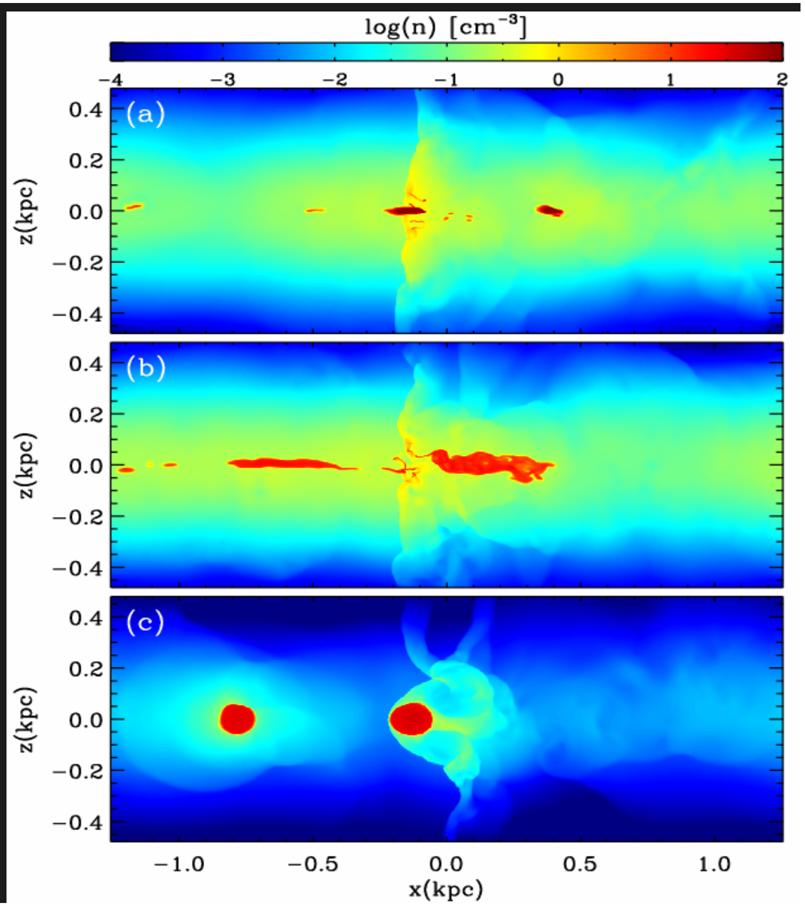

Vertical Velocity Dispersion

- Diffuse medium ($n < 1\ cm^{-3}$)
  - $\sigma_z \sim 1.9$ km/s (model A); $\sigma_z \sim 1.9$ km/s (model B); $\sigma_z \sim 4.0$ km/s (model C)
  - effect of the modified EOS is insignificant for diffuse medium
- Dense medium ($n > 1\ cm^{-3}$)
  - $\sigma_z \sim 0.3$ km/s (model A); $\sigma_z \sim 1.0$ km/s (model B); $\sigma_z \sim 2.2$ km/s (model C)
  - Episodic increase of σ_z in model C is due to collisions of dense clumps.

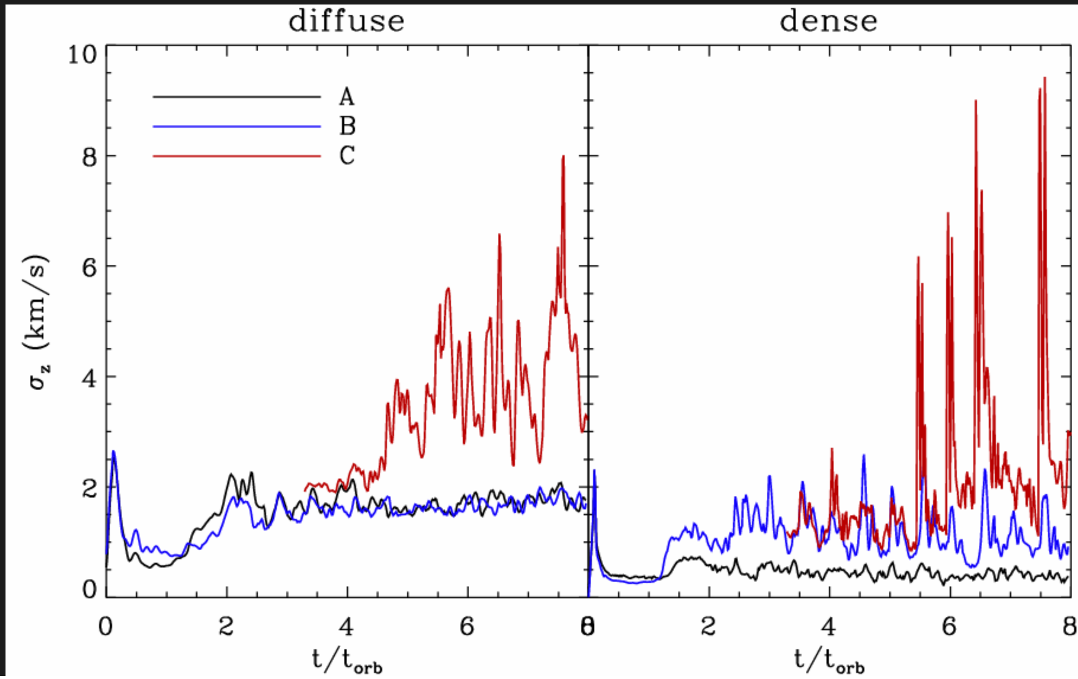

Summary

- In disks with spiral features,
  - Magneto-Jeans instability is active to develop spiral-arm substructures such as spurs and giant clouds, as long as the gas is "warm" with effective velocity dispersion of 10 km s^{-1}.
    - With reduced shear and enhanced magnetic fields, MJI is very efficient inside spiral arms.
    - $\lambda_{spur} \sim 10\, \lambda_{J,\, arm}$ (in 3D models)
  - Shock flapping motions naturally feed random gas motions
    - Difficult to excite gaseous motions in the vertical direction.
  - Spiral shocks with TI allow phase transitions of the gas
    - Warm to cold at the shock
    - Cold to warm at the postshock expansion zone.
  - Strong cooling at the spiral shock allows the formation of dense clumps even without self-gravity.